CRYSTAL GROWTH & DESIGN

Article

pubs.acs.org/crystal

Architectural Diversity for Anion-Mediated Self-Assembly of Four Pairs of Silver(I) Polymeric Isomers Having Linear and *V*-Shaped Imidazole/Thiophene/Imidazole Bridging Spacers

Bin Hu,[†,‡] Tao Tao,[†] Zheng-Yang Bin,[†] Yu-Xin Peng,[†] Bin-Bin Ma,[†] and Wei Huang*[,†]

[†]State Key Laboratory of Coordination Chemistry, Nanjing National Laboratory of Microstructures, School of Chemistry and Chemical Engineering, Nanjing University, Nanjing 210093, P. R. China

[‡]School of Environmental and Chemical Engineering, Nanchang Hangkong University, Nanchang, Jiangxi 330063, P. R. China

Supporting Information

ABSTRACT: A pair of linear and V-shaped acceptor−donor−acceptor (A−D−A) thiophene-based diazole structural isomers [i.e., 2,5-di(1*H*-imidazol-1-yl)thiophene (L^1) and 3,4-di(1*H*-imidazol-1-yl)thiophene (L^2)] have been used as bidentate bridging ligands to build Ag(I) fluorescent and semiconducting coordination polymers in the presence of different counterions. X-ray single-crystal diffraction analyses for eight complexes **1**−**8** reveal that they are four pairs of polymeric isomers formulated as $\{[Ag(L^1)(CF_3COO)]\}_n$ (**1**), $\{[Ag(L^2)(CF_3COO)]\}_n$ (**2**), $[Ag(L^1)(NO_3)]_n$ (**3**), $\{[Ag(L^2)(NO_3)]\cdot(H_2O)\}_n$ (**4**), $[Ag(L^1)(ClO_4)]_n$ (**5**), $\{[Ag(L^2)](ClO_4)\}_n$ (**6**), $\{[Ag(L^1)(CH_3CN)](PF_6)\}_n$ (**7**), and $\{[Ag(L^2)](PF_6)\cdot(CH_3CN)\}_n$ (**8**). They exhibit abundant structural diversity, namely, a one-dimensional (1D) dimeric chain **1**, a double-strand helix **2**, a cosinelike chain **3**, wavelike chains **4** and **8**, linear chains **5** and **7**, and a zigzag chain **6** because of the alterations of conformation for μ_2 bridging ligands L^1 and L^2 (cis/cis, cis/trans, and trans/trans) and the participancy of different counterions (CF_3COO^-, NO_3^-, ClO_4^-, and PF_6^-). It is noted that weak Ag(I)−thiophene coordinative bonds are observed in the case of **7** with the Ag−S distance of 3.057(4) Å, which lead to a 13.8× enhancement of solid-state conductivity in comparison with the semiconducting single crystal of **8** at room temperature.

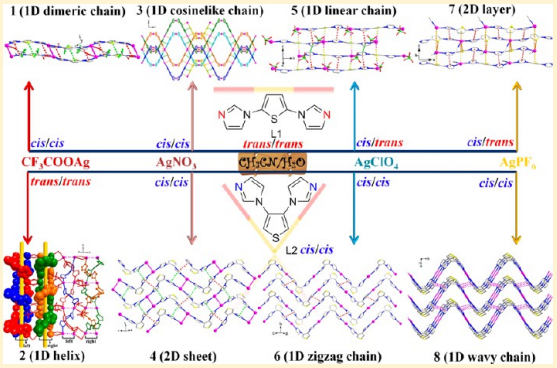

INTRODUCTION

Over the past decades, considerable efforts have been devoted to the theoretical prediction and the control of structures of metal coordination polymers (MCPs)[1] not only for their fascinating structural architectures but also for their attractive semiconducting,[2] luminescent,[3] optoelectronic,[4] and catalytic properties.[5] Many dedicated structural features of coordination polymers can be realized by supramolecular arrays exploiting rigid linear components, secondary building units, and elaborately chosen metal centers to construct. However, there are still many other factors which may affect the architectural engineering, since the final structures are also controlled by the pH value,[6] reaction temperature,[7] solvent system,[8] the conformation and shape of organic building blocks,[9] and the counterion.[10]

Ag(I) ion tends to form stable d^{10} closed-shell electronic configuration and low coordination number (2−4) exhibiting diverse coordination geometries (linear, trigonal, and tetrahedral coordination geometry), which has caused Ag(I) coordination polymers to have received much attention.[11] In addition, Ag(I) ion is apt to form Ag−Ag, Ag−π, and Ag···S contacts, which help to improve the related properties in the studies of optoelectronic materials.[2a] However, it will be usually unpredictable to control the final supramolecular architectures with the participation of diverse organic ligands. So the rational design, precise control, and systematic comparison of the supramolecular architectures by simply changing the conformation and shape of organic building blocks and counterions of silver(I) salts are still great challenges to chemists.

To date, linear and V-shaped aromatic heterocyclic ligands combining imidazole and thiophene rings into one molecule have been rarely explored in the investigations on constructing metal coordination polymers.[12] Actually, bent organic ligands (containing V-shaped ones) are good candidates for generating helical chains, cages, and other unprecedented polymeric structures, which demonstrate significant differences compared with the corresponding linear ligands.[9a] However, systematic comparisons of using a pair of thiophene-centered structural isomers to prepare a series of Ag(I) coordination polymers have never been explored for the investigation on supramolecular isomerism in the coordination polymers.

Received: October 23, 2013
Revised: November 25, 2013
Published: November 27, 2013

In this work, a pair of linear and V-shaped structural isomers with one central thiophene and two side imidazole rings, namely, 2,5-di(1*H*-imidazol-1-yl)thiophene (L^1) and 3,4-di(1*H*-imidazol-1-yl)thiophene (L^2), was used as bridging ligands to react with different Ag(I) salts (CF_3COO^-, NO_3^-, ClO_4^-, and PF_6^-) by the solvent evaporation method, and four pairs of polymeric isomers of silver(I) coordination polymers have been structurally and spectrally characterized and compared. They are formulated as $\{[Ag(L^1)(CF_3COO)]\}_n$ (**1**), $\{[Ag(L^2)(CF_3COO)]\}_n$ (**2**), $[Ag(L^1)(NO_3)]_n$ (**3**), $\{[Ag(L^2)(NO_3)]\cdot(H_2O)\}_n$ (**4**), $\{[Ag(L^1)(ClO_4)]\}_n$ (**5**), $[Ag(L^2)(ClO_4)]_n$ (**6**), $\{[Ag(L^1)(CH_3CN)](PF_6)\}_n$ (**7**), and $\{[Ag(L^2)](PF_6)\cdot(CH_3CN)\}_n$ (**8**), where abundant structural diversity has been observed because of the alterations of the shape and conformation for the μ_2 bridging ligands and the participancy of counterions. More interestingly, weak Ag(I)−thiophene coordinative bonds are observed in the case of **7** with the Ag−S distance of 3.057(4) Å, which lead to the 13.8× enhancement of solid-state conductivity in comparison with the semiconducting single crystal of **8** at room temperature.

EXPERIMENTAL SECTION

Materials and Measurements. The linear and V-shaped A−D−A thiophene-based diazole structural isomers 2,5-di(1*H*-imidazol-1-yl)thiophene (L^1) and 3,4-di(1*H*-imidazol-1-yl)thiophene (L^2) were prepared from 2,5-dibromothiophene and 3,4-dibromothiophene via literature methods.[12a] The light yellow needlelike single crystals of L^1 suitable for X-ray diffraction determination were grown from a solution of $CHCl_3$ by slow evaporation in air at room temperature. The syntheses of MCPs **1**−**8** were carried out in the dark environment to avoid photodecomposition. All other reagents were of analytical grade from commercial sources and were used without any further purification. Elemental analyses were measured with a Perkin-Elmer 1400C analyzer. Infrared spectra (FT-IR, 4000−400 cm^{-1}) were collected on a Nicolet FT-IR 170X spectrophotometer at room temperature using KBr plates. Luminescence spectra were recorded on a Hitachi 850 fluorescent spectrophotometer at room temperature. Powder X-ray diffraction (PXRD) measurements were performed on a Philips X'pert MPD Pro X-ray diffractometer, using Cu Kα radiation (λ = 0.15418 nm), in which the X-ray tube was operated at 40 kV and 40 mA at room temperature. TG−DSC experiments were carried out by a NETZSCH STA449C thermogravimetric analyzer instrument in the nitrogen flow from 27 to 700 °C, at a heating rate of 10.0 °C·min^{-1}.

Caution! Although no problem was encountered in all our experiments, transition metal perchlorates are potentially explosive and should be handled in small quantities.

*Syntheses of Four Pairs of Ag(I) Polymeric Isomers **1**−**8**.* *$\{[Ag(L^1)(CF_3COO)]\}_n$ (**1**).* A mixture of $AgCF_3COO$ (22.1 mg, 0.1 mmol) and L^1 (21.6 mg, 0.1 mmol) was stirred in a mixture of acetonitrile and H_2O (10 mL, v/v = 4/1). Then aqueous NH_3 solution (25%, 0.5 mL) was added dropwise into the mixture to give a clear solution at room temperature. The resultant solution was allowed to evaporate slowly in darkness at room temperature for several days and colorless single crystals suitable for X-ray diffraction determination were isolated after several days. Yield = 68% (based on L^1). Anal. Calcd for $C_{12}H_8AgF_3N_4O_2S$: C, 32.97; H, 1.84; N, 12.82%. Found: C, 32.54; H, 1.69; N, 12.96%. Main FT-IR absorptions (KBr pellets, cm^{-1}): 3416 (b, s), 3117 (m), 2361 (s), 2338 (m), 1680 (s), 1580 (m), 1514 (w), 1481 (m), 1433 (w), 1292 (w), 1213 (m), 1180 (m), 1126 (m), 1047 (m), 926 (w), 808 (w), 725 (m), and 652 (w).

*$\{[Ag(L^2)(CF_3COO)]\}_n$ (**2**).* Complex **2** was prepared in the same way as that of complex **1**, except that ligand L^2 (21.6 mg, 0.1 mmol) was used instead of L^1. Colorless block single crystals for X-ray analysis were obtained in a yield of 65% (based on L^2). Anal. Calcd for $C_{12}H_8AgF_3N_4O_2S$: C, 32.97; H, 1.84; N, 12.82%. Found C, 32.85; H, 1.90; N, 12.77%. Main FT-IR absorptions (KBr pellets, cm^{-1}): 3444 (b, s), 3107 (m), 1680 (m), 1529 (m), 1384 (s), 1335 (m), 1129 (s), 1069 (m), 1043 (m), 822 (m), and 779 (m).

*$[Ag(L^1)(NO_3)]_n$ (**3**).* Complex **3** was prepared in the same way as that of complex **1**, except that $AgNO_3$ (17.0 mg, 0.1 mmol) was used instead of $AgCF_3COO$. Colorless block single crystals for X-ray analysis were obtained in a yield of 67% (based on L^1). Anal. Calcd for $C_{10}H_{10}AgN_5O_4S$: C, 29.72; H, 2.49; N, 17.33%. Found: C, 29.96; H, 2.31; N, 17.12%. Main FT-IR absorptions (KBr pellets, cm^{-1}): 3115 (m), 2363(m), 2338(m), 1578 (m), 1524(w), 1495 (m), 1348(s), 1306(s), 1246(m), 1111(w), 1047 (m), 939 (w), 816 (w), 741 (w), and 648 (w).

*$\{[Ag(L^2)](NO_3)\cdot(H_2O)\}_n$ (**4**).* Complex **4** was prepared in the same way as that of complex **3**, except that ligand L^2 (21.6 mg, 0.1 mmol) was used instead of L^1. Colorless block single crystals for X-ray analysis were obtained in a yield of 63% (based on L^2). Anal. Calcd for $C_{10}H_{10}AgN_5O_4S$: C, 29.72; H, 2.49; N, 17.33%. Found: C, 29.62; H, 2.50; N, 17.24%. Main FT-IR absorptions (KBr pellets, cm^{-1}): 3441 (b, s), 3058 (m), 1535 (m), 1384 (s), 1330 (m), 1250 (m), 1217 (m), 1110 (m), 1072 (m), 938 (m), 827 (m), 746 (m), and 656 (m).

*$\{[Ag(L^1)(ClO_4)]\}_n$ (**5**).* Complex **5** was prepared in the same way as that of complex **1**, except that $AgClO_4$ (20.7 mg, 0.1 mmol) was used instead of $AgCF_3COO$. Colorless block single crystals for X-ray analysis were obtained in yield of 71% (based on L^1). Anal. Calcd for $C_{10}H_8AgClN_4O_4S$: C, 28.36; H, 1.90; N, 13.23%. Found: C, 28.17; H, 1.63; N, 13.42%. Main FT-IR absorptions (KBr pellets, cm^{-1}): 3115 (m), 2361(m), 2338(m), 1645(w), 1576 (m), 1524(w), 1493 (m), 1313 (s), 1267 (w), 1240 (w), 1138 (m), 1113 (w), 1049 (m), 924 (w), 829 (m), 808 (m), 756 (w), 729 (w), 650 (w), and 500 (m).

*$\{[Ag(L^2)](ClO_4)\}_n$ (**6**).* Complex **6** was prepared in the same way as that of complex **5**, except that ligand L^2 (21.6 mg, 0.1 mmol) was used instead of L^1. Colorless block single crystals for X-ray analysis were obtained in a yield of 77% (based on L^2). Anal. Calcd for $C_{10}H_8AgClN_4O_4S$: C, 28.36; H, 1.90; N, 13.23%. Found: C, 28.41; H, 1.78; N, 13.30%. Main FT-IR absorptions (KBr pellets, cm^{-1}): 3440 (br), 3134 (m), 1531 (s), 1387 (m), 1326 (m), 1243 (m), 1091 (s), 941 (m), 823 (m), 743 (m), and 621 (m).

*$\{[Ag(L^1)(CH_3CN)](PF_6)\}_n$ (**7**).* Complex **7** was prepared in the same way as that of complex **1**, except that $AgPF_6$ (25.3 mg, 0.1 mmol) were used instead of $AgCF_3COO$. Colorless block single crystals for X-ray analysis were obtained in a yield of 68% (based on L^1). Anal. Calcd for $C_{12}H_{11}AgF_6N_5PS$: C, 28.25; H, 2.17; N, 13.73%. Found: C, 28.37; H, 2.09; N, 13.54%. Main FT-IR absorptions (KBr pellets, cm^{-1}): 3450 (br), 3111 (m), 3088 (w), 1630 (w), 1576 (m), 1520 (w), 1485 (m), 1294 (w), 1244 (w), 1213 (w), 1109 (w), 1045 (w), 833 (s), 746 (w), 648 (w), 619 (w), and 559 (m).

*$\{[Ag(L^2)](PF_6)\cdot(CH_3CN)\}_n$ (**8**).* Complex **8** was prepared in the same way as that of complex **7**, except that ligand L^2 (21.6 mg, 0.1 mmol) was used instead of L^1. Colorless block single crystals for X-ray analysis were obtained in a yield of 72% (based on L^2). Anal. Calcd for $C_{12}H_{11}AgF_6N_5PS$: C, 28.25; H, 2.17; N, 13.73%. Found: C, 28.13; H, 2.24; N, 13.93%. Main FT-IR absorptions (KBr pellets, cm^{-1}): 3452 (br), 3113 (m), 3055 (m), 1630 (w), 1528 (m), 1491 (w), 1408 (w), 1333 (w), 1310 (w), 1242 (w), 1113 (w), 1068 (w), 1042 (w), 835 (vs), 760 (w), 743 (w), 654 (w), and 559 (m).

X-ray Data Collection and Structural Determination. All single-crystal samples were glue-covered and mounted on glass fibers for data collection on a Bruker SMART APEX CCD diffractometer using graphite monochromated Mo Kα radiation (λ = 0.71073 Å) at room temperature. The collected data were reduced by using the program SAINT[17] and empirical absorption corrections were done by the SADABS program. The crystal systems were determined by Laue symmetry and the space groups were assigned on the basis of systematic absences by using XPREP. The structures were solved by direct method and refined by the least−squares method. All nonhydrogen atoms were anisotropically refined,[18] and all hydrogen atoms were inserted in the calculated positions assigned fixed isotropic thermal parameters at 1.2 times the equivalent isotropic U of the atoms to which they are attached (1.5 times for the methyl groups and nitrogen and oxygen atoms) and allowed to ride on their respective parent atoms. Three fluorine atoms (F1, F2, and F3) of CF_3COO^- in

dx.doi.org/10.1021/cg401581q | *Cryst. Growth Des.* 2014, 14, 300−309

Table 1. Crystal Data and Structure Refinements for Ligand L^1 and Ag(I) Coordination Polymers 1−8

compound	L^1	1	2	3	4	5	6	7	8
formula	$C_{10}H_8N_4S$	$AgC_{12}H_8F_3N_4O_2S$	$AgC_{12}H_8F_3N_4O_2S$	$Ag_2C_{20}H_{16}N_{10}O_6S_2$	$AgC_{10}H_{10}N_5O_4S$	$AgC_{10}H_8ClN_4O_4S$	$AgC_{10}H_8ClN_4O_4S$	$AgC_{12}H_{11}F_6N_5PS$	$AgC_{12}H_{11}F_6N_5PS$
fw	216.26	437.16	437.16	772.29	404.16	423.59	423.59	510.16	510.16
T (K)	291(2)	291(2)	291(2)	291(2)	291(2)	291(2)	291(2)	291(2)	291(2)
crystal system	monoclinic	monoclinic	monoclinic	monoclinic	monoclinic	monoclinic	monoclinic	orthorhombic	monoclinic
space group	$P2_1/c$	$C2/c$	$C2/c$	$P2/c$	$P2_1/n$	$P2_1/c$	$P2_1/n$	$Pbca$	$P2_1/m$
a (Å)	9.2946(11)	12.9222(13)	26.457(12)	13.254(2)	9.4803(14)	9.5081(6)	9.3474(11)	13.123(1)	6.434(4)
b (Å)	10.8638(12)	10.3009(13)	8.367(4)	7.3495(13)	9.4473(14)	13.1649(9)	10.4189(12)	20.4789(16)	15.763(2)
c (Å)	10.7403(12)	22.021(3)	15.214(9)	13.555(2)	15.163(2)	13.5056(10)	14.0975(16)	13.487(1)	8.963(4)
α (°)	90	90	90	90	90	90	90	90	90
β (°)	113.337(1)	104.940(3)	119.368(4)	110.680(3)	94.868(2)	127.054(1)	97.117(2)	90	100.968(18)
γ (°)	90	90	90	90	90	90	90	90	90
V (Å^3)	995.8(2)	2832.1(6)	2935(3)	1235.3(3)	1353.2(3)	1349.17(16)	1362.4(3)	3624.6(5)	892.4(7)
Z/D_{calcd} (g/cm^3)	4/1.410	8/2.051	8/1.979	2/2.076	4/1.984	4/2.085	4/2.065	8/1.870	2/1.899
F(000)	336	1712	1712	760	800	832	832	2000	500
μ (Mo Kα, mm^{-1})	0.293	1.619	1.563	1.816	1.668	1.867	1.849	1.380	1.402
refs collected/unique	5300/1963	7692/2490	6899/2563	6575/2178	6513/2383	7431/2377	6688/2386	19084/3184	5638/1998
reflections [$I > 2\sigma$ (I)]	1336	2105	1947	1826	1707	2143	1564	2449	1572
parameters	169	236	208	177	190	190	218	235	138
R_1 [$I > 2\sigma$ (I)]	0.0376	0.0367	0.0555	0.0601	0.0366	0.0355	0.0411	0.0490	0.0516
wR_2 (all data)	0.0732	0.0927	0.1788	0.1729	0.0803	0.1106	0.1268	0.1615	0.1537
S	0.91	1.07	1.07	1.19	0.96	1.06	0.95	1.12	1.06
max/min $\Delta\rho$ (e Å^{-3})	0.21/−0.26	0.87/−0.66	2.11/−0.91	2.70/−2.54	0.75/−0.72	0.82/−0.99	0.51/−0.88	0.70/−0.77	0.95/−1.23

$R_1 = \Sigma||Fo| - |Fc||/\Sigma|Fo|$, $wR_2 = [\Sigma[w(Fo^2 - Fc^2)^2]/\Sigma w(Fo^2)^2]^{1/2}$

dx.doi.org/10.1021/cg401581q | Cryst. Growth Des. 2014, 14, 300−309

Table 2. Selected Bond Distances (Å) and Bond Angles (deg) in Ligand L^1 and Ag(I) Coordination Polymers 1−8

L^1		1		2		3		4	
C1−N1	1.302(3)	Ag1−N1	2.153(4)	Ag1−N2	2.136(5)	Ag1−N1	2.149(6)	Ag1−N2	2.108(4)
C1−N2	1.365(2)	Ag1−N4^a	2.142(4)	Ag1−N4^a	2.136(5)	Ag1−N1^a	2.149(6)	Ag1−N4^a	2.111(3)
C2−N1	1.368(3)	Ag1−O1	2.565(4)	Ag1−O1	2.702(5)	Ag1−O4	2.736(13)	Ag1−O3	2.808(4)
C3−N2	1.373(3)	Ag1−Ag1^b	3.365(1)	Ag1−O1^b	2.760(5)	Ag2−N4	2.117(6)	Ag1−Ag1^b	3.172(1)
C4−N2	1.408(2)	Ag1^c−N4	2.142(4)	Ag1−Ag1^c	3.566(2)	Ag2−N4^b	2.117(6)		
C4−S1	1.719(2)					Ag2−O2	2.971(10)		
C7−N3	1.408(2)								
C7−S1	1.723(2)	N4^a−Ag1−N1	169.6(2)	N2−Ag1−N4^a	165.6(2)	N1−Ag1−N1^a	175.4(3)	N2−Ag1−N4^a	169.4(2)
C8−N3	1.383(2)	N4^a−Ag1−O1	103.3(1)	N2−Ag1−O1	100.9(2)	N1−Ag1−O4	87.7(2)	N2−Ag1−O3	86.1(1)
C9−N4	1.375(3)	N1−Ag1−O1	84.5(1)	N4^a−Ag1−O1	93.5(2)	N1^a−Ag1−O4	87.7(2)	N4^a−Ag1−O3	84.1(1)
C10−N3	1.362(2)	N4^a−Ag1−Ag1^b	108.0(1)	N2−Ag1−O1^b	86.7(2)	N4−Ag2−O2	88.2(2)	N2−Ag1−Ag1^b	97.2(1)
C10−N4	1.306(2)	N1−Ag1−Ag1^b	81.9(1)	N4^a−Ag1−O1^b	95.8(2)	N4^b−Ag2−O2	91.8(2)	N4^a−Ag1−Ag1^b	89.5(1)
		O1−Ag1−Ag1^b	57.5(1)	O1−Ag1−O1^b	83.4(2)			O3−Ag1−Ag1^b	109.1(1)
				N2−Ag1−Ag1^c	80.4(1)				
				O1−Ag1−Ag1^c	128.3(1)				
				O1^b−Ag1−Ag1^c	147.4(1)				

5		6		7		8	
Ag1−N1	2.143(3)	Ag1−N2	2.082(5)	Ag1−N1	2.149(4)	Ag1−N2^a	2.095(3)
Ag1−N4^a	2.137(3)	Ag1−N4^a	2.088(5)	Ag1−N4^a	2.156(4)	Ag1−N2	2.095(3)
Ag1−O1	2.639(4)			Ag1−N5	2.455(6)	Ag1−F1	2.942(5)
N1−Ag1−N4^a	162.4(2)	N2−Ag1−N4^a	176.0(2)	N1−Ag1−N4^a	156.6(2)	N2^a−Ag1−F1	92.9(2)
N1−Ag1−O1	87.8(1)			N1−Ag1−N5	100.7(2)	N2−Ag1−F1	87.1(2)
N4^a−Ag1−O1	109.3(1)			N4^a−Ag1−N5	102.6(2)		

^{a}Symmetry codes: 1, −1/2 + x, 3/2 − y, −1/2 + z; 2, −x, 1 + y, 0.5 − z; 3, 1 − x, y, 1/2 − z; 4, −1/2 + x, 1/2 − y, 1/2 + z; 5, x, −1 + y, z; 6, −1/2 + x, 1/2 − y, 1/2 + z; 7, 1 + x, y, z; 8, 1 − x, 1 − y, 1 − z. ^{b}Symmetry codes: 1, 1/2 − x, 3/2 − y, 1 − z; 2, −x, 2 − y, 1 − z; 3, 2 − x, −y, −z; 4, 1 − x, 1 − y, 2 − z; 5, x, 1 + y, z; 6, 1/2 + x, 1/2 − y, −1/2 + z; 7, −1 + x, y, z. ^{c}Symmetry codes: 1, 1/2 + x, 3/2 − y, 1/2 + z; 2, −x, y, 0.5 − z.

1 are found disordered over two positions with the site occupancy factors of 0.64(1):0.36(1). Three oxygen atoms (O2, O3, and O4) of ClO_4^- in **6** are found disordered over two positions with the site occupancy factors of 0.47(3):0.53(3). One fluorine atom (F3) of PF_6^- in **8** is found disordered over two positions with the site occupancy factors of 0.49(2):0.51(2). All calculations were carried out on a PC computer with the SHELXTL PC program package,[19] and the molecular graphics were drawn by using XSHELL and DIAMOND software. Details of the data collection and refinement for ligand L^1 and MCPs **1**−**8** are given in Table 1, and the selective bond lengths and angles are listed in Table 2. Hydrogen bonding data are listed in Table SI1 of the Supporting Information.

RESULTS AND DISCUSSION

Syntheses and Spectral Characterizations. Linear and V-shaped structural isomers L^1 and L^2 were prepared via the carbon−nitrogen bond cross-coupling reactions between imidazole and 2,5-dibromothiophene/3,4-dibromothiophene using the same Ullmann method.[12] It is obvious that the V-shaped molecule has a worse delocalized π system than the linear one because of the stronger steric hindrance between the two side imidazole rings, which results in larger dihedral angles between the central thiophene and the side imidazole rings in ligand L^2. In comparison with the α,α'-thiophene-based heterocyclic aromatic compounds, which are generally in the linear configuration, the β,β'-thiophene derivatives preferably adopt the V-shaped configuration. On the other hand, since the monovalent Ag(I) ion has lower coordination number (2−4) compared with divalent Co(II), Ni(II), and Zn(II) ions (4−6) in the solid state, lower dimensions of MCPs can be expected. Furthermore, compared with the first-row Co(II), Ni(II), and Zn(II) transition-metal ions, a larger monovalent Ag(I) ion is much easier to be polarized, which can significantly facilitate the electron transport within the MCPs. So in this work, we design and prepare a pair of linear and V-shaped A−D−A[20] structural isomers and use them as organic building blocks to react with the Ag salts in order to construct corresponding MCPs. In addition, four types of counterions (CF_3COO^-, NO_3^-, ClO_4^-, and PF_6^-) are used to finely tune the final self-assembled structures. As a result, four pairs of polymeric isomers of MCPs **1**−**8** have been obtained successfully, which exhibit different supramolecular architectures because of the distinguishing shape and configuration of structural isomers L^1 and L^2, as well as the participancy of different counterions.

The luminescence properties of two ligands and their eight Ag(I) coordination polymers in the solid state have been explored. As can be seen in Figure 1, ligand L^1 exhibits a stronger fluorescence emission than that of ligand L^2, indicative of better planarity for 2,5-substituted thiophene rings. However, the fluorescence of two ligands is much weaker than their Ag(I) coordination polymers **1**−**8**, which can be attributed to the

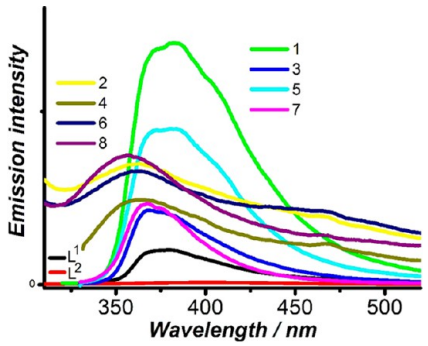

Figure 1. Solid-state fluorescence emission spectra of L^1−L^2 and Ag(I) coordination polymers **1**−**8** at room temperature.

dx.doi.org/10.1021/cg401581q | Cryst. Growth Des. 2014, 14, 300−309

effective increase of polymeric rigidity and crystal packing by forming Ag(I)-N coordinative bonds and $\pi-\pi$ stacking interactions. Furthermore, MCPs of linear ligand L^1 (**1**, **3**, **5**, and **7**) have fluorescence emission peaks varying from 368 to 379 nm, while those of V-shaped ligand L^2 (**2**, **4**, **6**, and **8**) are in the range of 356−362 nm. In our case, only complexes **1** and **5** show slightly red-shifted emission λ_{max} compared with corresponding bridging ligand L^1, which can be ascribed to the more excellent planarity with smaller dihedral angles after Ag(I) ion coordination in their solid-state structures. In contrast, V-shaped ligand L^2 has a worse delocalized π-system than linear ligand L^1 due to the stronger steric hindrance effect, which will result in larger dihedral angles between the central thiophene and side imidazole rings after Ag(I) ion complexation. So the blue-shifted emission λ_{max} has been observed for ligand L^2 based MCPs, which can be further verified by their single-crystal structures.

The phase purity of all eight MCPs in this work has been further confirmed by the PXRD patterns (Figure S2 of the Supporting Information), in which the simulated patterns generated from the results of single-crystal diffraction data and as-synthesized ones are almost identical, demonstrating good phase purity of the products. Thermogravimetry analysis and simultaneous differential scanning calorimeter (TG−DSC) experiments of MCPs **7** and **8** were performed in N_2 atmosphere, and the results are illustrated in Figure S3 of the Supporting Information. Complexes **7** and **8** are stable up to 284 and 327 °C, respectively, and after that, their host frameworks begin to decompose. Meanwhile, MCP **7** has a weight-loss process for the coordinating acetonitrile molecules after 102 °C with a mass change of 7.82% (calcd 8.05%). In contrast, the removal of solvent acetonitrile molecules can be observed in the ranges of 50−185 °C for MCP **8** with a weight loss of 8.15% (calcd 8.05%).

Structural Description of Linear Thiophene-Based Diazole L^1. The molecular structure of L^1 with the atom-numbering scheme is shown in Figure 2a. It crystallizes in the monoclinic $P2_1/c$ space group, and the two side imidazole rings are not coplanar to the central thiophene ring. Instead, they are staggered at each side of the thiophene plane with the dihedral angles of 37.7(2) and 33.8(2)°, respectively, adopting the trans/trans conformation. In the crystal packing of L^1, $\pi-\pi$ stacking interactions are found between the central thiophene rings and the two side imidazole rings from adjacent molecules with centroid−centroid separations of 3.761(2) and 3.806(2) Å.

Structural Description of $\{[Ag(L^1)(CF_3COO)]\}_n$ (1) and $\{[Ag(L^2)(CF_3COO)]\}_n$ (2). Single-crystal X-ray determination of complex **1** indicates that the asymmetric unit contains one ligand L^1, one CF_3COO^- anion, and one Ag(I) ion. As shown in Figure 2b, the central Ag1 ion exhibits approximately *T*-shaped coordination geometry defined by two imidazole *N*-donors (N1 and N4A, $-1/2 + x$, $3/2 - y$, $-1/2 + z$) from two L^1 ligands and one *O*-donor from the CF_3COO^- anion. The CF_3COO^- anions in **1** act as monodentate terminal ligands with the Ag−O bond length of 2.565(4) Å, while the other two Ag−N bond distances are 2.142(4) and 2.153(4) Å. It is noteworthy that the two imidazole rings of ligand L^1 in **1** adopt the cis/cis conformation relative to the central thiophene units, which is different from that in the free ligand. Moreover, the dihedral angles between the central thiophene ring and its two side imidazole rings for ligand L^1 are significantly decreased to 4.7(1) and 2.0(1)° after metal−ion complexation. Ligand L^1 serves as a μ_2 spacer linking adjacent Ag(I) ions to form a one-dimensional (1D) polymeric chain.

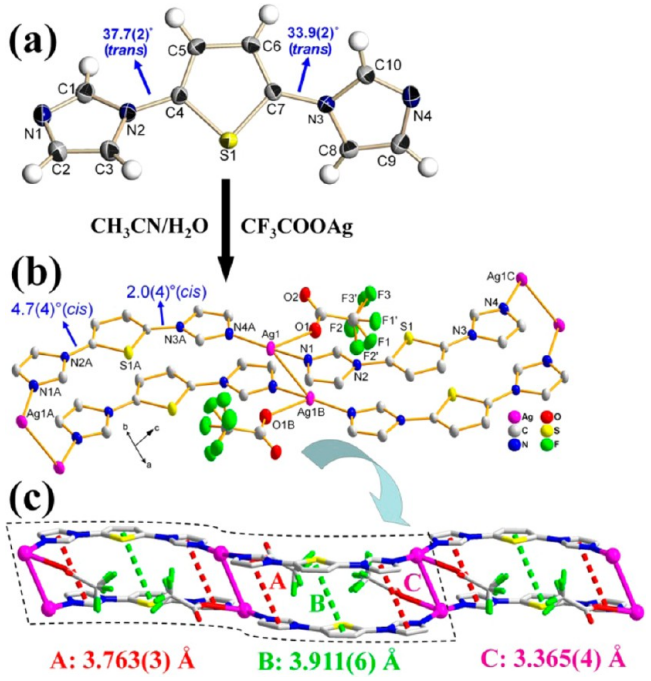

Figure 2. (a and b) ORTEP diagrams (30% thermal probability) of the molecular structures of L^1 and **1** with the atom-numbering scheme. (c) Perspective view of the 1D dimeric polymer in **1**, containing the Ag−Ag and $\pi-\pi$ stacking interactions.

A novel 1D wavelike dimeric packing structure is constituted in **1** (Figure 2c), where fused $\pi-\pi$ stacking interactions are observed between all the aromatic rings and their counterparts with the centroid−centroid distances of 3.763(3) and 3.911(6) Å, respectively. Moreover, the Ag−Ag distance between neighboring two 1D polymeric chains is 3.365(4) Å, which is shorter than the van der Waals distance for Ag−Ag (3.40 Å).[13] Additionally, intrachain O−H···O and C−H···F hydrogen bonds (Table SI1 of the Supporting Information) are present cooperatively to further stabilize the wavelike dimeric packing structure in **1**.

In contrast, complex **2** shows a two-dimensional (2D) supramolecular structure made up of 1D double-strand helices via double μ_2 oxygen bridges from two CF_3COO^- anions. As shown in Figure 3a, the coordination geometry of every Ag(I) center is a distorted tetrahedron comprised of two N atoms from two L^2 ligands and two O atoms from two trifluoroacetate anions. One oxygen atom of each trifluoroacetate group acts as a μ_2 bridge to link adjacent two silver ions forming a parallelogram dinuclear Ag_2O_2 unit. The corresponding Ag···Ag separation is 4.077(2) Å and the N−Ag−N angle [165.6(1)°] deviates from linearity because of the coordination of trifluoroacetate anions to the silver centers. However, the dihedral angles between the two side imidazole rings and the central thiophene ring in the bidentate bridging ligand L^2 are 62.1(5) and 69.4(5)°, respectively, which are much larger than those in **1**. Ligand L^2 adopts the trans/trans conformation in **2**, which is consistent with that in the free L^2 ligand.[12b] In addition, the dihedral angle between the two coordinated imidazole rings at each side of the Ag(I) center is 81.7(5)°, which is obviously different from the essentially coplanar configuration [6.6(4)°] in **1**.

dx.doi.org/10.1021/cg401581q | Cryst. Growth Des. 2014, 14, 300−309

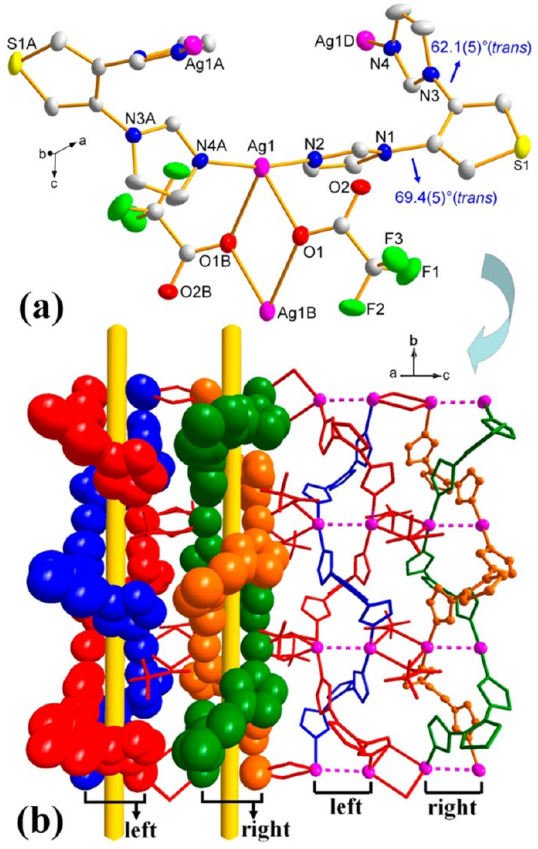

Figure 3. (a) ORTEP drawing of **2** showing 30% ellipsoid probability (hydrogen atoms and water molecules are omitted for clarity). (b) Perspective view of the 2D coordination polymer in **2** extended from 1D alternately arranged left- and right-handed double-strand helices.

Every L^2 ligand links adjacent Ag(I) ions as a μ_2 spacer, forming a 1D helical chain, where the nearest nonbonding Ag···Ag distance connected by L^2 is 9.095(2) Å. The aforementioned dinuclear silver(I) units are further linked by very weak Ag···Ag interactions [3.566(2) Å], along the crystallographic *c* axis (Figure 3b). The Ag···Ag···Ag angle is 168.9(1)°, and the dihedral angle between the neighboring Ag_2O_2 parallelograms is 77.8(2)°. It is worthwhile to mention that the double-strand helices are interwoven down the crystallographic *b* axis, in which each helical cycle is composed of three silver(I) ions bridged by two L^2 ligands with a pitch of 16.734(2) Å. Furthermore, the left-handed (red and blue chains shown in the space-filling representation) and the right-handed double-strand helices (green and orange) belonging to vicinal dinuclear silver(I) units are alternately arranged via double Ag−O−Ag bridges, constructing a novel 2D racemic helical framework (Figure 3b). By comparing the Ag(I) polymeric isomers of **1** and **2**, it is concluded that distinguishable dimeric and double-strand helical coordination polymers are constructed by using a pair of structural isomers L^1 and L^2 with different molecular configuration as the μ_2 bridging ligands.

Structural description of $\{[Ag(L^1)](NO_3)\}_n$ (3) and $\{[Ag(L^2)(NO_3)]\cdot(H_2O)\}_n$ (4). When NO_3^- is used to replace CF_3COO^-, a 1D cosinelike polymeric chain **3** and a 2D supramolecular network **4** have been obtained. As shown in Figure 4a, there are two kinds of Ag(I) centers in **3**. One is coordinated by two N atoms from two distinct imidazole rings and one weakly coordinated oxygen atom from the nitrate anion with the N1−Ag1−N1A (1 − *x*, *y*, 1/2 − *z*) bond angle of 175.4(3)°, forming [2 + 1] *T*-shaped coordination geometry. The other is linearly two-coordinated by two nitrogen atoms from two adjacent imidazole rings with the N4−Ag2−N4B (2 − *x*, −*y*, −*z*) bond angle of 180.0°. All L^1 ligands in **3** display the same cis/cis configuration with the dihedral angles between the neighboring aromatic rings of 16.3(6) and 26.2(6)°,

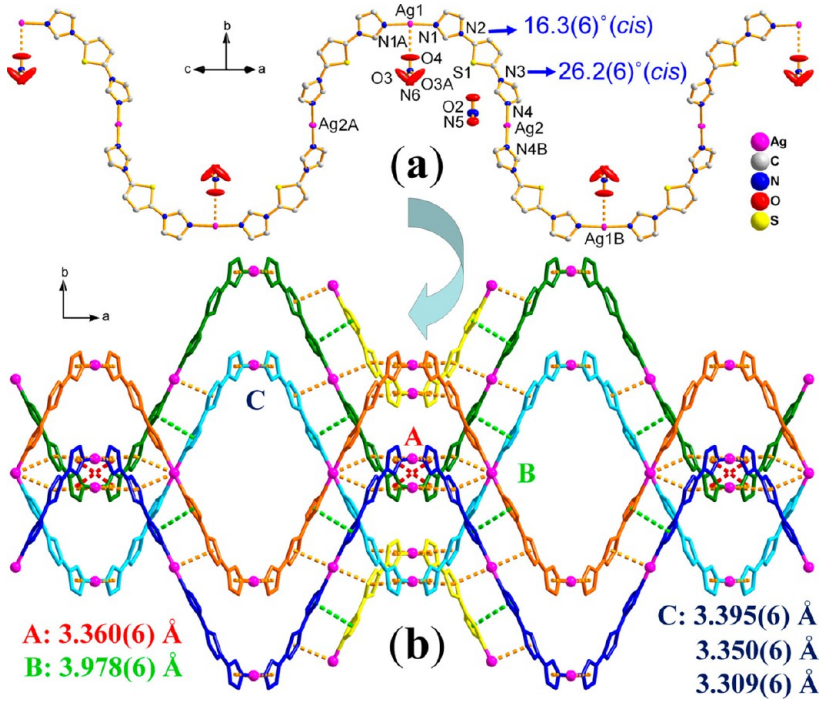

Figure 4. (a) ORTEP diagram (30% thermal probability) of **3** with the atom-numbering scheme, hydrogen atoms are omitted for clarity. (b) Perspective view of the 1D cosinelike Ag(I) coordination polymer in 3, together with the Ag−π and π−π stacking interactions.

dx.doi.org/10.1021/cg401581q | *Cryst. Growth Des.* 2014, 14, 300−309

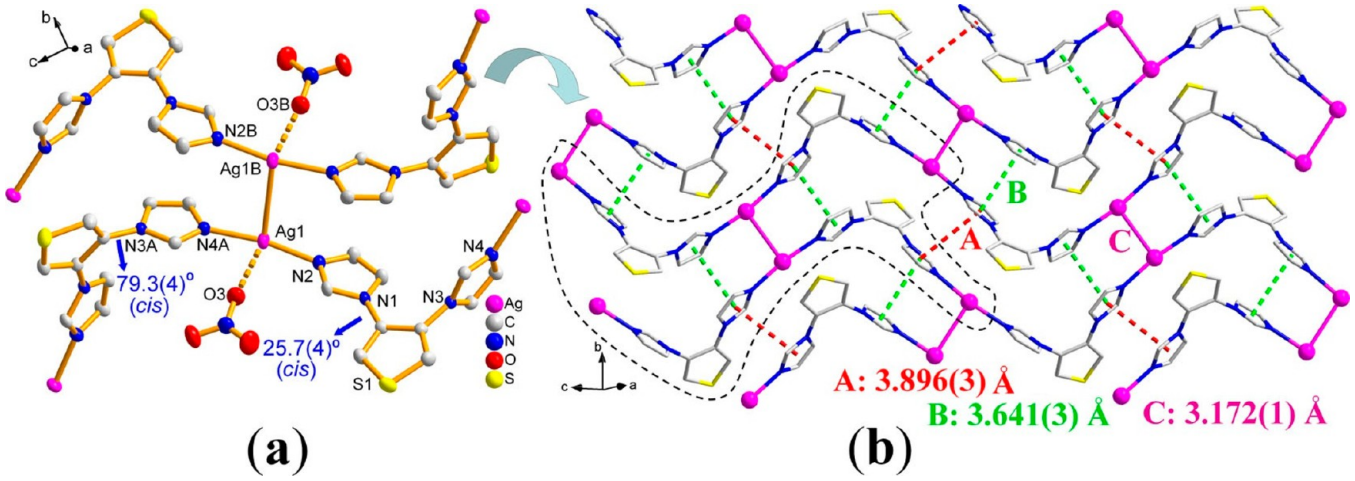

Figure 5. (a) ORTEP drawing of **4** showing 30% ellipsoid probability (hydrogen atoms and water molecules are omitted for clarity). (b) Perspective view of the 2D supramolecular network in **4** containing the Ag−Ag and $\pi-\pi$ stacking interactions.

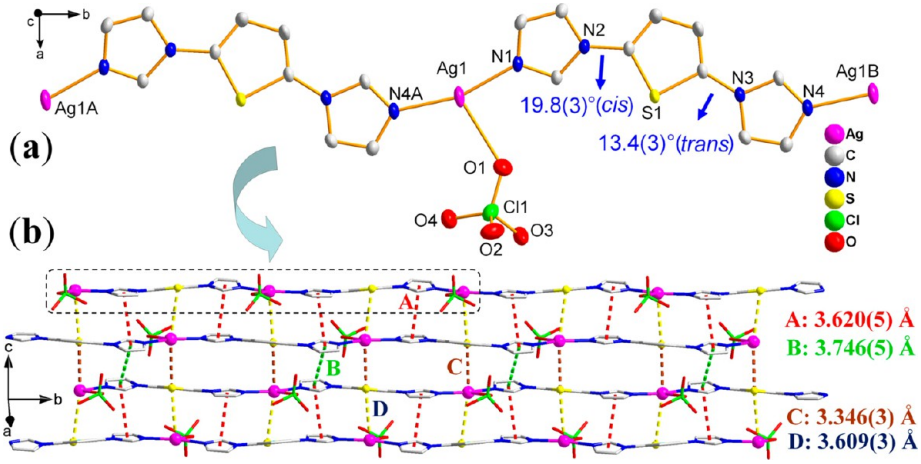

Figure 6. (a) ORTEP diagram (30% thermal probability) of **5** with the atom-numbering scheme (hydrogen atoms are omitted for clarity). (b) Perspective view of the 2D supramolecular framework involving the Ag···S, Ag−π, and $\pi-\pi$ stacking interactions.

respectively. A 1D cosinelike polymeric chain is thus formed in the case of **3**. Furthermore, adjacent 1D cosinelike polymeric chains are connected by multiple Ag···π interactions ranging from 3.309(6) to 3.395(6) Å and $\pi-\pi$ stacking interactions of 3.360(6) and 3.978(6) Å, generating a 2D supramolecular framework (Figure 4b).

In the 2D coordination polymer **4**, there are one Ag(I) ion, one L^2 ligand, one NO_3^- anion, and one free water molecule in the asymmetric unit. As shown in Figure 5a, similar to Ag1 in complex **3**, every Ag(I) center in complex **4** displays a [2 + 1] *T*-shaped coordination mode, where the N2−Ag1−N4A (−1/2 + *x*, 1/2 − *y*, 1/2 + *z*) bond angle is measured as 169.4(2)° and the dihedral angle between two imidazole rings at each side of Ag(I) center is 87.6(4)°. The two imidazole rings in the cis/cis ligand L^2 are staggered at each side of the thiophene plane with the dihedral angles of 25.7(4) and 79.3(4)°, respectively. Every bidentate bridging ligand L^2 links adjacent two Ag(I) centers, forming a wavy 1D infinite MCP. The 1D infinite MCPs are further connected into a 2D supramolecular network by the Ag−Ag interactions [3.172(1) Å] as well as the $\pi-\pi$ stacking interactions between adjacent side imidazole rings of the L^2 ligands with the centroid−centroid separations of 3.641(3) and 3.896(3) Å (Figure 5b), where a 38-membered $Ag_6(L^2)_4$ metallocyclic ring is included.

Structural Description of $\{[Ag(L^1)(ClO_4)]\}_n$ (5) and $\{[Ag(L^2)](ClO_4)\}_n$ (6). When ClO_4^- is used to mediate the self-assembly, quasi-linear and zigzag 1D coordination polymers **5** and **6** are yielded, respectively. As shown in Figure 6a, the central Ag(I) ion in **5** has a [2 + 1] *T*-shaped coordination fashion, which is analogous to that of complex **4**. The related Ag−N distances are 2.143(3) and 2.137(3) Å and the N−Ag−N angle is 162.4(2)°, while the Ag−O bond length is much longer at 2.639(4) Å. The two imidazole rings related to the central thiophene adopt the cis/trans conformation in ligand L^1 with the dihedral angles of 19.8(3) and 13.4(3)° between them. Different from the 1D dimeric and cosinelike coordination polymers **1** and **3**, a quasi-linear 1D coordination polymer is built in **5**, where every ligand L^1 adopts an antiparallel bridging mode to link adjacent Ag(I) centers. It is noted that the 1D MCPs are further connected by strong Ag···S [3.346(3) and 3.609(3) Å], Ag···π [3.620(5) Å], and $\pi-\pi$ stacking interactions [3.746(5) Å], as depicted in Figure 6b.

In comparison with the polymeric isomer of **5**, a different 1D zigzag coordination polymer is formed in **6**. Every Ag(I) ion in **6** is linearly two-coordinated by two nitrogen atoms from two L^2 ligands with the N−Ag−N bond angle of 176.0(2)°, and the dihedral angle between these two imidazole rings is 76.1(5)°, as shown in Figure 7a. The two imidazole rings in ligand L^2 are

dx.doi.org/10.1021/cg401581q | *Cryst. Growth Des.* 2014, 14, 300−309

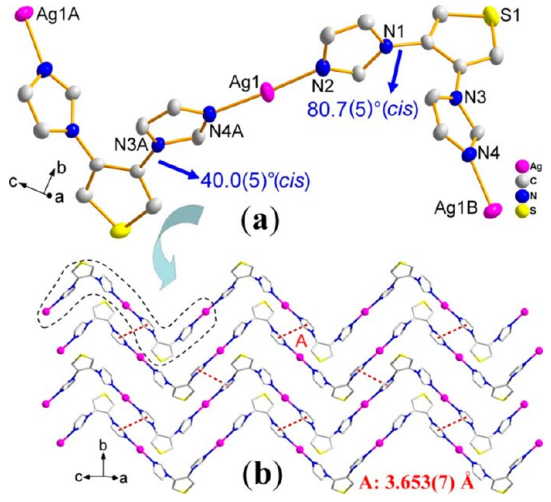

Figure 7. (**a**) ORTEP drawing of **6** showing 30% ellipsoid probability (hydrogen atoms and ClO_4^- anions are omitted for clarity) and hydrogen atoms and are omitted for clarity. (**b**) Perspective view of the 1D zigzag chains in **6** connected by the $\pi-\pi$ stacking interactions.

also not coplanar to the central thiophene ring with the dihedral angles of 80.7(5) and 40.0(5)°, respectively. Every ligand L^2 in **6** shows the cis/cis conformation bridging adjacent Ag(I) ions into a 1D zigzag coordination polymer. There are interchain $\pi-\pi$ stacking interactions between the side imidazole rings in ligands L^2 from adjacent 1D chains, and the centroid–centroid separation between them is 3.653(7) Å, extending the 1D chains into a 2D sheet framework along the crystallographic *b* axis (Figure 7b).

Structural Description of $\{[Ag(L^1)(CH_3CN)](PF_6)\}_n$ (7) and $\{[Ag(L^2)](PF_6)\cdot(CH_3CN)\}_n$ (8). More supramolecular architectures can be achieved when the PF_6^- anion is used to replace the CF_3COO^- anion in **1** and **2**, ClO_4^- anion in **3** and **4**, and NO_3^- anion in **5** and **6**. The asymmetric unit of **7** consists of one Ag(I) cation, one bidentate bridging ligand L^1, one coordinated acetonitrile molecule, and one PF_6^- anion. Like those in **3** and **5**, the central Ag(I) ion in **7** has a [2 + 1] *T*-shaped coordination fashion (Figure 8a). The corresponding Ag–N distances are 2.149(4) and 2.156(4) Å, but the other Ag–N distance with the acetonitrile molecule is the shortest one [2.455(6) Å] in this paper. Accordingly, the smallest N–Ag–N angle of 156.6(2)° is found in the case of **7**, indicating the presence of the strongest Ag–solvent/anion coordinative bonds. The two side imidazole rings in ligand L^1 adopt the cis/trans conformation relative to the central thiophene rings, where the dihedral angles between adjacent aromatic rings are 25.9(4) and 25.3(4)°, respectively. Neighboring Ag(I) ions are connected by μ_2 bridging ligands L^1, forming another 1D coordination polymer in **7**. It is interesting to mention that unusual Ag(I)–thiophene coordinative bonds[14] are observed with the Ag–S bond length of 3.057(4) Å, connecting the 1D chains into a 2D network. Furthermore, the 1D chains are condensely packed with the assistance of Ag···π [3.337(5) and 3.784(5) Å] and $\pi-\pi$ stacking interactions [3.530(6) Å], besides the aforementioned Ag–S coordinative bonds (Figure 8b).

X-ray diffraction analysis of **8** reveals that one Ag(I) ion, half of ligand L^2, a PF_6^- anion, and one solvent acetonitrile molecule are present in the asymmetric unit. As shown in Figure 9a, the coordination geometry of Ag(I) center is a two-coordinate straight-line fashion by two nitrogen atoms from two L^2 ligands with the N–Ag–N bond angle of 180.0(2)°. However, very weak coordinative bonds are observed between the central Ag(I) ion and two fluorine atoms of two PF_6^- anions with the Ag–F bond length of 2.942(5) Å. Similarly, a 1D coordination polymer comes into being in **8** by means of the linkage of μ_2-bridging ligand L^2 with the cis/cis conformation (Figure 9b), where the dihedral angles between the adjacent aromatic rings in ligand L^2 are the same as 77.1(3)°. The 1D MCPs are further extended into a 2D

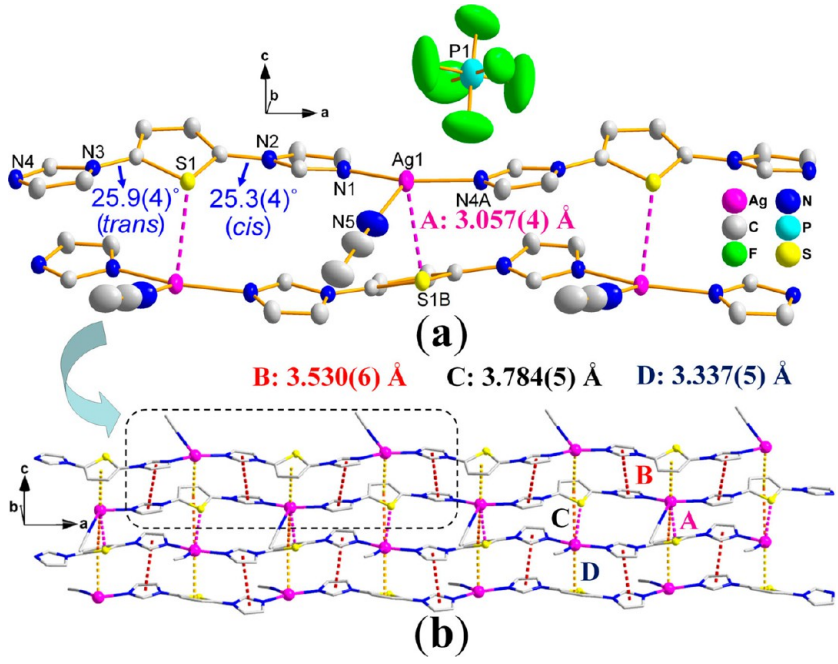

Figure 8. (**a**) ORTEP drawing of **7** showing 30% ellipsoid probability (hydrogen atoms are omitted for clarity). (**b**) Perspective view of the 2D supramolecular framework in **7** containing the Ag–S, Ag–π, and $\pi-\pi$ stacking interactions.

dx.doi.org/10.1021/cg401581q | *Cryst. Growth Des.* 2014, 14, 300–309

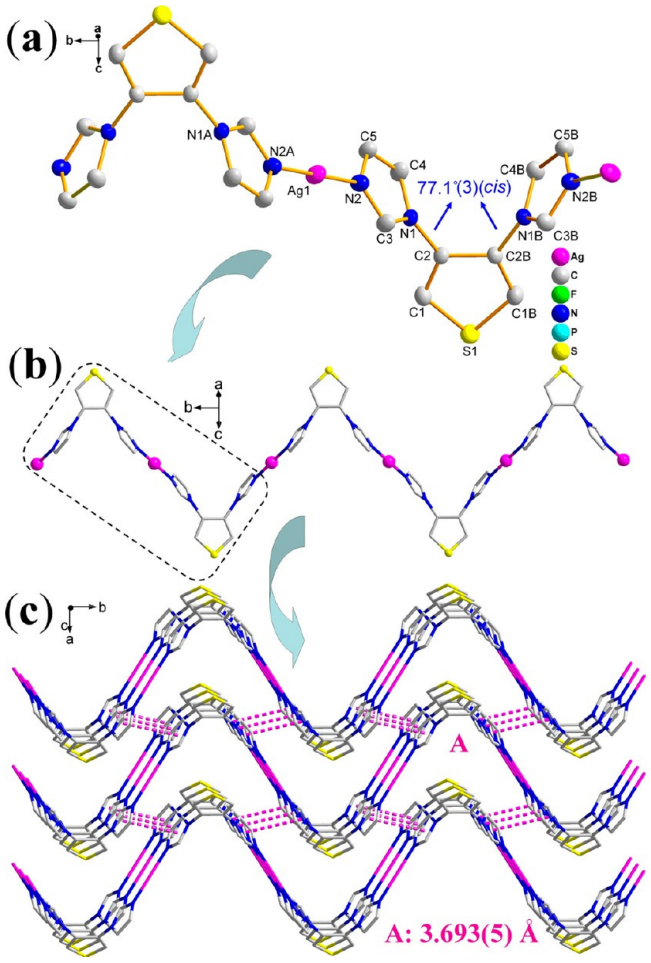

Figure 9. (a) ORTEP drawing of **8** showing 30% ellipsoid probability (hydrogen atoms and acetonitrile molecule are omitted for clarity). (b) Perspective view of the 1D wavy coordination polymer in **8**. (c) Perspective view of the 2D supramolecular framework connected by the $\pi-\pi$ stacking interactions in **8**.

supramolecular framework via the $\pi-\pi$ stacking interactions [3.693(5) Å] between adjacent imidazole rings from different 1D chains (Figure 9c).

Single-Crystal Conductivity for Silver(I) Coordination Polymers. Generally speaking, V-shaped ligand L^2 based Ag(I) complexes have worse delocalized π-systems than the linear ligand L^1 based ones, owing to larger dihedral angles between the central thiophene and side imidazole rings, so better electrical conductivity of compounds can be predicted for the latter ones. In consideration of the formation of 1D dimeric polymeric chain in **1** and closely stacked 2D frameworks in **5** and **7** by means of Ag−O, Ag−Ag, and Ag−S bonded contacts as well as Ag$\cdots\pi$ and $\pi-\pi$ stacking interactions, good solid-state conductivity of these semiconducting coordination polymers are expected. So we tried to grow big single crystals of them and determine their solid-state conductivity, together with MCP **8** for comparison. As shown in Figure 10, solid-state conductivity measurement on the single-crystal samples of **1**, **5**, **7**, and **8** has been measured at room temperature. The $I-V$ curves are recorded between a pair of gold electrodes in the voltage range from −10 to 10 V at room temperature via the Lake Shore CRX-4K four-probe system. No obvious conductance is found in the cases of ligands L^1 and L^2, indicative of their insulating behavior. In contrast, the $I-V$ curves of **1**, **5**, **7**, and **8** are almost linear (ohmic) and the current can reach as high as the μA order in the measured voltage range, indicative of typical semiconducting properties.[15] The most possible reason for the enhancement of solid-state conductivity after metal−ion complexation lies in the increase of additional electron-transfer pathways via $\pi-\pi^*$, Ag$\cdots\pi$/Ag$\cdots\pi^*$, Ag−Ag, Ag$\cdots$S, and Ag−S interactions, which can provide effective electron transportation among the adjacent polymeric units.[2a,16]

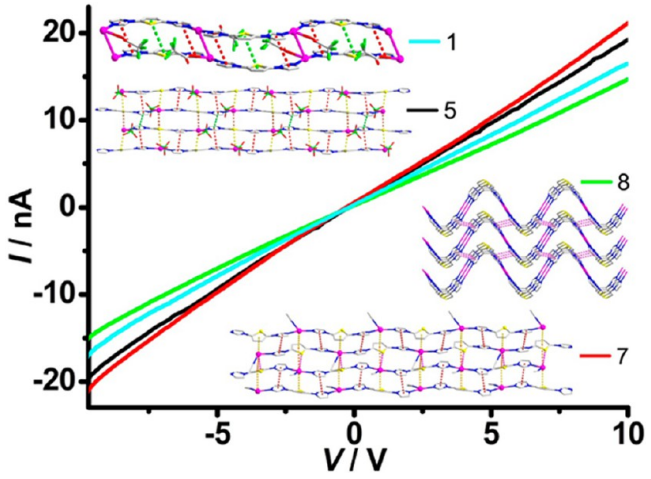

Figure 10. (a) $I-V$ curves for complexes **1**, **5**, **7**, and **8** in the voltage range from −10 to 10 V at room temperature.

Linear fitting of the reproducible $I-V$ curves gave an average conductivity of 2.64×10^{-5} S·m^{-1} for **1**, 2.56×10^{-5} S·m^{-1} for **5**, 4.80×10^{-5} S·m^{-1} for **7**, and 3.47×10^{-6} S·m^{-1} for **8**. The measured single-crystal conductivity of **1**, **5**, **7**, and **8** is believed to be consistent with their crystal packing structures, which have been discussed in the structural description part. That is to say, linear ligand L^1 involved MCPs have better solid-state conductivity than V-shaped ligand L^2 involved ones, which is originated from the conformational discrepancy of structural isomers L^1 and L^2. For example, **7** has a 13.8× enhancement of solid-state conductivity compared with that of **8**. In addition, among ligand L^1 involved MCPs **1**, **5**, and **7**, the presence of weak Ag−S-bonded contacts in **7** can slightly strengthen the packing among 1D polymeric chains and hence increase the solid-state conductivity.

■ CONCLUSION

In summary, supramolecular isomerism and anion-mediated self-assembly in the coordination polymers are studied in this work by using a pair of structural isomers L^1 and L^2 as μ_2 bridging ligands containing the common imidazole/thiophene/imidazole skeleton but with distinct molecular shapes. Distinguishable 1D Ag(I) coordination polymers having multifarious architectural diversity, namely, a dimeric chain **1**, a double-strand helix **2**, a cosinelike chain **3**, wavelike chains **4** and **8**, linear chains **5** and **7**, and a zigzag chain **6**, have been constructed in the presence of different counterions (CF_3COO^-, NO_3^-, ClO_4^-, and PF_6^-), where ligands L^1 and L^2 show variable cis/cis, cis/trans, and trans/trans configuration. These Ag(I) fluorescent and semiconducting coordination polymers **1**−**8** are four pairs of polymeric isomers, where the $\pi-\pi$, Ag$\cdots\pi$, and Ag$\cdots$S interactions are widely found in their crystal packing. It is worth mentioning that uncommon Ag(I)−thiophene coordinative bonds are observed in the case of **7** with the Ag−S distance of 3.057(4) Å, which leads to a

dx.doi.org/10.1021/cg401581q | Cryst. Growth Des. 2014, 14, 300−309

13.8× enhancement of solid-state conductivity at room temperature in comparison with the semiconducting single crystal **8**.

■ ASSOCIATED CONTENT

Supporting Information

Hydrogen bonds, PXRD, and TG−DSC data for related compounds are attached. CCDC numbers 963157−963165 contain the supplementary crystallographic data of nine compounds in this paper. These data can also be obtained free of charge, upon request, at www.ccdc.cam.ac.uk/conts/retrieving.html [or from the Cambridge Crystallographic Data Centre, 12 Union Road, Cambridge CB2 1EZ, U.K.; fax (Internet) +44−1223/336−033; e-mail request@ccdc.cam.ac.uk]. This material is available free of charge via the Internet at http://pubs.acs.org.

■ AUTHOR INFORMATION

Corresponding Author

*E-mail: whuang@nju.edu.cn. Tel: +86-25-83686526. Fax: +86-25-83314502.

Notes

The authors declare no competing financial interest.

■ ACKNOWLEDGMENTS

This work was financially supported by the Major State Basic Research Development Programs (Grants 2013CB922101 and 2011CB933300), the National Natural Science Foundation of China (Grant 21171088), the Natural Science Foundation of Jiangsu Province (Grant BK20130054), the China Postdoctoral Science Foundation (Grant 2012M511720), and the Qing Lan Project.

■ REFERENCES

(1) (a) DeCola, L. *Molecular Wires: From Design to Properties*; Springer-Verlag: Berlin, 2005; Vol. *257*, pp 1−170. (b) *Molecular Materials*; Bruce, D. W., Walton, R. I., O'Hare, D., Eds.; Wiley-VCH: Hoboken, 2010; pp 1−374. (c) Chakrabarty, R.; Mukherjee, P. S.; Stang, P. J. *Chem. Rev.* **2011**, *111*, 6810−6918. (d) Masoomi, M. Y.; Morsali, A. *Coord. Chem. Rev.* **2012**, *256*, 2921−2943. (e) Zhang, J. Y.; Su, C. Y. *Coord. Chem. Rev.* **2013**, *257*, 1373−1408.

(2) (a) Zheng, S. L.; Zhang, J. P.; Wong, W. T.; Chen, X. M. *J. Am. Chem. Soc.* **2003**, *125*, 6882−6883. (b) Xu, Z. T. *Coord. Chem. Rev.* **2006**, *250*, 2745−2757. (c) Tachikawa, T.; Choi, J. R.; Fujitsuka, M.; Majima, T. *J. Phys. Chem. C* **2008**, *112*, 14090−14101.

(3) (a) Kishimura, A.; Yamashita, T.; Aida, T. *J. Am. Chem. Soc.* **2005**, *127*, 179−183. (b) Barbieri, A.; Accorsi, G.; Armaroli, N. *Chem. Commun.* **2008**, 2185−2193. (c) He, Y. H.; Feng, Y. L.; Lan, Y. Z.; Wen, Y. H. *Cryst. Growth Des.* **2008**, *8*, 3586−3594.

(4) (a) Crassous, J.; Reau, R. *Dalton Trans.* **2008**, 6865−6876. (b) Klapshina, L. G.; Douglas, W. E.; Grigoryev, I. S.; Korytin, A. I.; Lavrentiev, S. A.; Lopatin, M. A.; Lukyanov, A. Y.; Semenov, V. V.; Gerbier, P.; Treushnikov, V. M. *J. Mater. Chem.* **2009**, *19*, 3668−3676. (c) Khajavi, H.; Gascon, J.; Schins, J. M.; Siebbeles, L. D. A.; Kapteijn, F. *J. Phys. Chem. C* **2011**, *115*, 12487−12493.

(5) (a) Song, F. J.; Wang, C.; Falkowski, J. M.; Ma, L. Q.; Lin, W. B. *J. Am. Chem. Soc.* **2010**, *132*, 15390−15398. (b) Wang, D. H.; Zhang, B. G.; He, C.; Wu, P. Y.; Duan, C. Y. *Chem. Commun.* **2010**, *46*, 4728−4730. (c) Kan, W. Q.; Liu, B.; Yang, J.; Liu, Y. Y.; Ma, J. F. *Cryst. Growth Des.* **2012**, *12*, 2288−2298. (d) Gonell, S.; Poyatos, M.; Peris, E. *Angew. Chem., Int. Ed.* **2013**, *52*, 7009−7013.

(6) (a) Wu, S. T.; Long, L. S.; Huang, R. B.; Zheng, L. S. *Cryst. Growth Des.* **2007**, *7*, 1746−1752. (b) Liu, F. R.; Wang, K. Z.; Bai, G. Y.; Zhang, Y. G.; Gao, L. H. *Inorg. Chem.* **2004**, *43*, 1799−1806. (c) Koo, C. K.; Lam, B.; Leung, S. K.; Lam, M. H. W.; Wong, W. Y. *J. Am. Chem. Soc.* **2006**, *128*, 16434−16435. (d) Zheng, H. Q.; Xing, L.; Cao, Y. Y.; Che, S. A. *Coord. Chem. Rev.* **2013**, *257*, 1933−1944.

(7) (a) Masaoka, S.; Tanaka, D.; Nakanishi, Y.; Kitagawa, S. *Angew. Chem., Int. Ed.* **2004**, *43*, 2530−2534. (b) Zheng, B.; Dong, H.; Bai, J. F.; Li, Y. Z.; Li, S. H.; Scheer, M. *J. Am. Chem. Soc.* **2008**, *130*, 7778−7779.

(8) (a) Huang, X. C.; Li, D.; Chen, X. M. *CrystEngComm* **2006**, *8*, 351−355. (b) Hush, N. S.; Reimers, J. R. *Coord. Chem. Rev.* **1998**, *177*, 37−60. (c) Hush, N. S.; Reimers, J. R. *Chem. Rev.* **2000**, *100*, 775−786. (d) Pedireddi, V. R.; Varughese, S. *Inorg. Chem.* **2004**, *43*, 450−457.

(9) (a) Dong, Y. B.; Xu, H. X.; Ma, J. P.; Huang, R. O. *Inorg. Chem.* **2006**, *45*, 3325−3343. (b) Li, C. Y.; Liu, C. S.; Li, J. R.; Bu, X. H. *Cryst. Growth Des.* **2007**, *7*, 286−295. (c) Deng, Z. P.; Zhu, L. N.; Gao, S.; Huo, L. H.; Ng, S. W. *Cryst. Growth Des.* **2008**, *8*, 3277−3284.

(10) (a) Schottel, B. L.; Chifotides, H. T.; Shatruk, M.; Chouai, A.; Perez, L. M.; Bacsa, J.; Dunbar, K. R. *J. Am. Chem. Soc.* **2006**, *128*, 5895−5912. (b) Wei, K. J.; Ni, J.; Gao, M.; Liu, Y. Z.; Liu, Q. L. *Eur. J. Inorg. Chem.* **2007**, 3868−3880. (c) Manzano, B. R.; Jalon, F. A.; Soriano, M. L.; Carrion, M. C.; Carranza, M. P.; Mereiter, K.; Rodriguez, A. M.; de la Hoz, A.; Sanchez-Migallon, A. *Inorg. Chem.* **2008**, *47*, 8957−8971.

(11) (a) Khlobystov, A. N.; Blake, A. J.; Champness, N. R.; Lemenovskii, D. A.; Majouga, A. G.; Zyk, N. V.; Schroder, M. *Coord. Chem. Rev.* **2001**, *222*, 155−192. (b) Meijboom, R.; Bowen, R. J.; Berners-Price, S. J. *Coord. Chem. Rev.* **2009**, *253*, 325−342. (c) Tao, T.; Lei, Y. H.; Peng, Y. X.; Wang, Y.; Huang, W.; Chen, Z. X.; You, X. Z. *Cryst. Growth Des.* **2012**, *12*, 4580−4587.

(12) (a) Wang, L.; Tao, T.; Fu, S. J.; Wang, C.; Huang, W.; You, X. Z. *CrystEngComm* **2011**, *13*, 747−749. (b) Fu, S. J.; Wang, L.; Tao, T.; Hu, B.; Huang, W.; You, X. Z. *CrystEngComm* **2011**, *13*, 6192−6199.

(13) (a) Venkataraman, D.; Du, Y. H.; Wilson, S. R.; Hirsch, K. A.; Zhang, P.; Moore, J. S. *J. Chem. Educ.* **1997**, *74*, 915−918. (b) Batsanov, S. S. *Inorg. Mater.* **2001**, *37*, 871−885.

(14) (a) Konaka, H.; Wu, L. P.; Munakata, M.; Kuroda-Sowa, T.; Maekawa, M.; Suenaga, Y. *Inorg. Chem.* **2003**, *42*, 1928−1934. (b) Dong, Y. B.; Geng, Y.; Ma, J. P.; Huang, R. Q. *Organometallics* **2006**, *25*, 447−462. (c) Zhao, L.; Mak, T. C. W. *Organometallics* **2007**, *26*, 4439−4448.

(15) Kittel, C. *Introduction to Solid State Physics*, 5th ed.; John Wiley & Sons: New York, 1976.

(16) (a) Shimizu, G. K. H.; Enright, G. D.; Ratcliffe, C. I.; Ripmeester, J. A.; Wayner, D. D. M. *Angew. Chem., Int. Ed.* **1998**, *37*, 1407−1409. (b) Blake, A. J.; Champness, N. R.; Hubberstey, P.; Li, W. S.; Withersby, M. A.; Schroder, M. *Coord. Chem. Rev.* **1999**, *183*, 117−138. (c) Ni, J.; Wei, K. J.; Liu, Y. Z.; Huang, X. C.; Li, D. *Cryst. Growth Des.* **2010**, *10*, 3964−3976. (d) Habata, Y.; Taniguchi, A.; Ikeda, M.; Hiraoka, T.; Matsuyama, N.; Otsuka, S.; Kuwahara, S. *Inorg. Chem.* **2013**, *52*, 2542−2549. (e) Sun, D.; Yang, C. F.; Xu, H. R.; Zhao, H. X.; Wei, Z. H.; Zhang, N.; Yu, L. J.; Huang, R. B.; Zheng, L. S. *Chem. Commun.* **2010**, *46*, 8168−8170.

(17) *SAINT v4 software reference manual*; Siemens Analytical X−Ray Systems, Inc.: Madison, Wisconsin, 2000.

(18) Sheldrick, G. M., *SHELXTL*, version 6.10; Bruker Analytical X-ray Systems: Madison, WI, 2000.

(19) *SAINT*, version 6.10; Bruker AXS, Inc.; Madison, WI, 2000.

(20) (a) Huang, W.; Tanaka, H.; Ogawa, T.; You, X. Z. *Adv. Mater.* **2010**, *22*, 2753−2758. (b) Hu, B.; Fu, S. J.; Xu, F.; Tao, T.; Zhu, H. Y.; Cao, K. S.; Huang, W.; You, X. Z. *J. Org. Chem.* **2011**, *76*, 4444−4456. (c) Tao, T.; Peng, Y. X.; Huang, W.; You, X. Z. *J. Org. Chem.* **2013**, *78*, 2472−2481. (d) Tao, T.; Ma, B. B.; Peng, Y. X.; Wang, X. X.; Huang, W.; You, X. Z. *J. Org. Chem.* **2013**, *78*, 8669−8679. (e) Tao, T.; Qian, H. F.; Zhang, K.; Geng, J.; Huang, W. *Tetrahedron* **2013**, *69*, 7290−7299.